A multireference perturbation method using non-orthogonal Hartree-Fock determinants for ground and excited states

Cite as: J. Chem. Phys. **139**, 174104 (2013); https://doi.org/10.1063/1.4827456
Submitted: 30 August 2013 . Accepted: 16 October 2013 . Published Online: 05 November 2013

Shane R. Yost, Tim Kowalczyk, and Troy Van Voorhis

A multireference perturbation method using non-orthogonal Hartree-Fock determinants for ground and excited states

Shane R. Yost, Tim Kowalczyk, and Troy Van Voorhis[a)]
Department of Chemistry, Massachusetts Institute of Technology, Cambridge, Massachusetts 02139-4307, USA

(Received 30 August 2013; accepted 16 October 2013; published online 5 November 2013)

In this article we propose the ΔSCF(2) framework, a multireference strategy based on second-order perturbation theory, for ground and excited electronic states. Unlike the complete active space family of methods, ΔSCF(2) employs a set of self-consistent Hartree-Fock determinants, also known as ΔSCF states. Each ΔSCF electronic state is modified by a first-order correction from Møller-Plesset perturbation theory and used to construct a Hamiltonian in a configuration interactions like framework. We present formulas for the resulting matrix elements between nonorthogonal states that scale as $N_{\text{occ}}^2 N_{\text{virt}}^3$. Unlike most active space methods, ΔSCF(2) treats the ground and excited state determinants even-handedly. We apply ΔSCF(2) to the H_2, hydrogen fluoride, and H_4 systems and show that the method provides accurate descriptions of ground- and excited-state potential energy surfaces with no single active space containing more than 10 ΔSCF states. © *2013 AIP Publishing LLC*. [http://dx.doi.org/10.1063/1.4827456]

I. INTRODUCTION

The properties of electronically excited states are crucial to various aspects of photochemistry, such as photoinduced electron transfer,[1,2] photocatalysis,[3,4] and photovoltaics.[5–7] Extensive efforts toward accurate and affordable electronic structure calculations of molecular excited states have led to significant improvements, but state-of-the-art approaches still cannot achieve sub-kcal mol^{-1} accuracy for excited states of any but the smallest of molecules.[8] One standard approach to computing excited states that only requires knowledge of the ground state wavefunction is linear response, in which excitation energies are identified with poles in the linear response function due to an electromagnetic perturbation.[9] However, linear response time-dependent Hartree-Fock (TDHF) provides limited accuracy for excited state energies and potential energy surfaces (PES), due to the neglect of dynamic correlation.[8] Its counterpart within density functional theory (DFT), linear response time-dependent DFT[10,11] (TDDFT) is a relatively affordable way to compute excited states, but its success with currently available exchange-correlation functionals is limited to certain classes of excited states. For well-behaved systems, accuracy of around 0.3 eV can be anticipated, but for charge transfer or Rydberg excitations, TDDFT shows significantly worse performance.[8] TDDFT fares even more poorly for excited state PES,[12,13] making it unreliable when searching for a reaction barrier or propagating dynamics in the excited state. The perennial issue with TDDFT and other DFT-based methods for excited states is the quality of the exchange-correlation functional. Efforts to improve on these approximations are ever ongoing,[14–17] but the roadmap to chemical accuracy for excited states in TDDFT remains blurry.

Wavefunction based methods building on the HF determinant, on the other hand, provide a more systematic way to generate high-quality ground and excited state wavefunctions. Due to the mean field approximation of HF theory, the HF wavefunction lacks all electron correlation. However, the static correlation can be recovered through the use of a multireference wavefunction, while the dynamic correlation is often more convenient to treat perturbatively.[18,19]

Perturbative treatments of dynamic correlation in quantum chemistry are usually based on the Møller-Plesset series.[20,21] Alternatively, one can extract dynamic correlation by applying single, double, and possibly higher order excitation operators to the ground state HF determinant. The improved single-reference ground state wavefunction is then a linear combination of these wavefunctions, the coefficients of which are obtained either by variational minimization, configuration interaction method (CI), or by solving a set of coupled coefficient equations, coupled-cluster method (CC).[22–24] In most cases, both CI and CC methods rapidly converge with respect to the order of the excitation operators, but the computational cost of including these higher-order excitations grows rapidly. Excited state methods rooted in this approach, such as equation-of-motion CC singles and doubles (CCSD),[25,26] second order approximate CC (CC2),[27,28] and quadratic CI singles and doubles (QCISD),[29] are even more computationally demanding and are unaffordable for excited state dynamics of more than ∼10-atom systems.

One drawback to single-reference methods is that they do not capture much static correlation, which can be important for systems with electronic degeneracies or small band gaps and which is required to obtain conical intersections. A number of multireference methods[19,30–33] have been developed to treat static correlation. A popular multireference method that efficiently captures static correlation, while reducing computational costs relative to full CI, is the complete active space self consistent field (CASSCF) method.[31] In state-specific CASSCF, CI is applied to an active space of molecular orbitals – usually a small number of occupied and

a)Electronic mail: tvan@mit.edu

virtual orbitals – instead of the full set. The CI coefficients and molecular orbitals in the active space are then optimized self-consistently to minimize the energy of the specified state. As with full CI, the cost of CASSCF grows combinatorially with the size of the active space. There exist various active space reduction strategies, such as restricted active space SCF (RASSCF),[32] to manage the balance between accuracy and computational cost. However, even with these tools, CAS methods are notoriously not black-box, and in practice, one needs to closely monitor the orbitals during PES scans and dynamics to ensure the consistency of the active space, and thus the accuracy of the calculation.[18,19] Because CASSCF captures most static correlation, it can produce qualitatively accurate potential energy surfaces even for conical intersections and nuclear dissociation. However, dynamic correlation enters into the CASSCF wavefunction only very gradually with respect to active space size.

To improve the description of dynamic correlation in multireference methods, Roos and co-workers extended CASSCF to include a second order perturbative correction to the CASSCF energies, resulting in the CASPT2 method.[34,35] There are several choices to be made in the construction of such a formalism, and so a variety of multireference perturbation theories have since been developed.[36–40] In CASPT2, the perturbation correction is applied after determining the CASSCF wavefunction ("diagonalize then perturb" approach), but this creates some ambiguity regarding what to define as the zeroth-order Hamiltonian for the perturbation theory.[41–44] Related methods such as multireference Møller-Plesset[38] and *n*-electron valence state perturbation theory[44] also follow the "diagonalize then perturb" philosophy and suffer from similar issues of defining the zeroth order Hamiltonian. A different approach based on the concept of an effective Hamiltonian which, when diagonalized, only gives some of the eigenvalues of the exact Hamiltonian[45–47] constitutes a "perturb then diagonalize" approach to multireference perturbation theory. Still other multireference methods use coupled-cluster theory instead of perturbation theory to add dynamic correlation to the total energy.[48–51] It is important to note that only "perturb then diagonalize" methods always preserve the structure of conical intersections.[52]

One issue for perturbation methods is that the perturbation series is not guaranteed to converge,[53–55] and in particular, second order perturbation theory can accumulate an unbounded error in the case of orbital near-degeneracies. Specifically, the perturbative energy will diverge whenever one of the orbitals outside the active space crosses one of the orbitals inside the active space; this is formally known as the intruder state problem.[56] This is still an issue that lacks a non-empirical solution.[57,58]

In treating both ground and excited states via CASPT2, an additional ambiguity arises in the prescription for the state averaging procedure used to select the optimal set of orbitals for all states. In particular, CASPT2 energies can depend significantly on the state averaging procedure used.[59] Finally, the accuracy of CASPT2 and other multireference perturbation theories depend on how large of a reference space is used, which is limited by computational resources. In the case of CASPT2 there are two computational bottlenecks: exponential scaling with respect to the number of active orbitals, and ninth-order scaling with respect to basis set size due to diagonalization of overlap matrices that depend on the third-order density matrix.[60,61]

Recently we[62] and others[63] have shown that the ΔSCF-DFT method[64] can often perform as well as TDDFT for a given choice of exchange-correlation functional. While the ΔSCF-DFT method only yields estimates of excited state properties of roughly the same quality as TDDFT,[62] the underlying strategy of ΔSCF-DFT suggests a unique opportunity to approach multireference problems from a new direction. In HF theory as in Kohn-Sham DFT, the ΔSCF approach can be used to enforce a selected non-Aufbau orbital occupation pattern during SCF energy minimization and converge onto an excited state determinant.

In this article, we introduce a "perturb then diagonalize" scheme rooted in the ΔSCF approach, which we call ΔSCF(2). In this scheme, the reference states are composed of the HF ground state wavefunction and a number of non-Aufbau HF excited state wavefunctions, each dressed with a perturbative correction in the spirit of second order Møller-Plesset perturbation theory (MP2). Due to the equal footing afforded to ground and excited states, the ΔSCF(2) method is well suited to treat both ground and excited states with a small number of reference wavefunctions.

In the remainder of this article, we first describe the ΔSCF(2) method in detail. Then we present applications to some minimal models of bond breaking and a conical intersection to assess its strengths and weaknesses.

II. THEORY

In the ΔSCF(2) method, the HF ground-state wavefunction and several non-Aufbau, stationary HF wavefunctions ($|\Phi_A^0\rangle \equiv |A^{(0)}\rangle$) are used as reference wavefunctions. Each determinant is obtained from a separate self-consistent HF calculation, resulting in an independent set of orbitals and eigenvalues. Static correlation in the ground and excited state wavefunctions ($|\Psi_n\rangle$) is expected to be reasonably well approximated by CI among these reference states:

$$|\Psi_n\rangle = \sum_A c_n^A |A\rangle. \tag{1}$$

To account for dynamic correlation outside of the reference space we apply second-order perturbation theory with the Fock operator as the zeroth-order Hamiltonian, which generates a first-order correction for each wavefunction,

$$|A\rangle = |A^{(0)}\rangle + |A^{(1)}\rangle \tag{2}$$

$$= |A^{(0)}\rangle + \frac{1}{4}\sum_{\substack{ij\\ab}} \alpha_{ij}^{ab} \big|A_{ij}^{ab}\big\rangle, \tag{3}$$

where $|A_{ij}^{ab}\rangle$ is the double excitation $i \to a, j \to b$ from $|A^{(0)}\rangle$ and its amplitude α_{ij}^{ab} is the standard PT2 amplitude for the $|A^{(0)}\rangle$ state,

$$\alpha_{ij}^{ab} = \frac{\langle ij||ab\rangle_A}{\epsilon_a^A + \epsilon_b^A - \epsilon_i^A - \epsilon_j^A}. \tag{4}$$

We use indices i, j, k, l for occupied orbitals, a, b, c, d for virtual orbitals, and p, q, r, s for either type of orbital. We also use index notation, so in the following expressions there is an implicit sum over repeated indices. Throughout this section we will use α_{ij}^{ab} and β_{ij}^{ab} as the PT2 amplitudes for states $|A^{(0)}\rangle$ and $|B^{(0)}\rangle$, respectively.

Each reference wavefunction is derived from an independent solution to the HF equations, with an independent set of optimized molecular orbitals (MOs); therefore the two-electron integrals and orbital energies depend on the reference wavefunction, as indicated in Eq. (4). In this sense, all states in ΔSCF(2) are determined at an equivalent level of theory, in contrast to the many multireference methods which generate excited states from constituent orbitals of the ground state, or from a single set of orbitals determined by state-averaging. The orbital relaxation that occurs for the non-Aufbau excited states during SCF convergence avoids the need to simultaneously optimize the orbitals and CI coefficients, or to determine the orbitals via state-averaging; instead, the orbitals for a given state are prescribed by a self-consistent minimization of that state's energy. Furthermore, in contrast to CASPT2, the choice of the zeroth order Hamiltonian in this basis is unambiguous, as will be described below. However, since the non-Aufbau wavefunctions are independently obtained solutions to the HF equations, orbitals from different states will generally be nonorthogonal.

The MP2-corrected ground state and non-Aufbau states define the basis of wavefunctions for the ΔSCF(2) method. In this "perturb then diagonalize" strategy, the ΔSCF(2) energies and wavefunctions are finally determined by computing the eigenvalues and eigenfunctions of the secular equation

$$\mathbf{Hc} = E\mathbf{Sc}, \tag{5}$$

where the Hamiltonian and overlap matrix elements are

$$\begin{aligned} H_{AB} &= \langle A|\hat{H}^A|B\rangle \\ &= \langle A^{(0)}|\hat{H}^A|B^{(0)}\rangle \\ &\quad + \frac{1}{2}(\langle A^{(0)}|\hat{H}^A|B^{(1)}\rangle + \langle A^{(1)}|\hat{H}^A|B^{(0)}\rangle), \end{aligned} \tag{6}$$

$$\begin{aligned} S_{AB} &= \langle \Phi_A|\Phi_B\rangle \\ &= \langle A^{(0)}|B^{(0)}\rangle + \frac{1}{2}(\langle A^{(0)}|B^{(1)}\rangle + \langle A^{(1)}|B^{(0)}\rangle). \end{aligned} \tag{7}$$

Since the perturbation has a different structure for each electronic state, off-diagonal terms in the Hamiltonian and overlap matrices do not possess a well-defined perturbation order. Nevertheless, the term $\langle A^{(1)}|\hat{H}^A|B^{(1)}\rangle$ can be considered higher-order in the sense that it depends on both first-order corrections and thus requires increased computational cost to evaluate. Based on these considerations, we truncate the perturbation expansion before this term. We multiply by a factor of 1/2 on the two terms on the RHS of Eqs. (6) and (7) so that the diagonal Hamiltonian matrix elements will reproduce the MP2 energy and the off-diagonal terms will be symmetric.

The zeroth-order like terms in Eqs. (6) and (7) are straightforward to evaluate, despite the nonorthogonality of molecular orbitals of $|A^{(0)}\rangle$ and $|B^{(0)}\rangle$.[9,33,65] To solve for the second order like terms in Eqs. (6) and (7), such as $\langle A^{(0)}|\hat{H}^A|B^{(1)}\rangle$, we first insert the identity $\mathbf{I} = |A^{(0)}\rangle\langle A^{(0)}| + |A_i^a\rangle\langle A_i^a| + |A_{ij}^{ab}\rangle\langle A_{ij}^{ab}| + |A_{ijk}^{abc}\rangle\langle A_{ijk}^{abc} + \ldots$ to get

$$\begin{aligned} \langle A^{(0)}|\hat{H}^A|B^{(1)}\rangle &= \langle A^{(0)}|\hat{H}^A|A^{(0)}\rangle\langle A^{(0)}|B^{(1)}\rangle \\ &\quad + \langle A^{(0)}|\hat{H}^A|A_i^a\rangle\langle A_i^a|B^{(1)}\rangle \\ &\quad + \langle A^{(0)}|\hat{H}^A\big|A_{ij}^{ab}\big\rangle\big\langle A_{ij}^{ab}\big|B^{(1)}\big\rangle \\ &\quad + \langle A^{(0)}|\hat{H}^A\big|A_{ijk}^{abc}\big\rangle\big\langle A_{ijk}^{abc}\big|B^{(1)}\big\rangle + \ldots. \end{aligned} \tag{8}$$

This gives an expression where the Hamiltonian matrix elements are now evaluated between orthogonal determinants and we just have overlap matrix elements between nonorthogonal determinants. The second term on the RHS of Eq. (8) is equal to zero because of Brillouin's theorem, and the last term on the RHS plus all of the higher order terms are zero because of the Slater-Condon rules.[22] Finally, we arrive at more manageable expressions for the second-order like terms in Eqs. (6) and (7):

$$\begin{aligned} \langle A^{(0)}|\hat{H}^A|B^{(1)}\rangle &= \frac{1}{4}E_A\langle A^{(0)}\big|B_{ij}^{ab}\big\rangle\beta_{ij}^{ab} \\ &\quad + \frac{1}{16}\langle kl\|cd\rangle_A\big\langle A_{kl}^{cd}\big|B_{ij}^{ab}\big\rangle\beta_{ij}^{ab}, \end{aligned} \tag{9}$$

$$\langle A^{(0)}|B^{(1)}\rangle = \frac{1}{4}\big\langle A^{(0)}\big|B_{ij}^{ab}\big\rangle\beta_{ij}^{ab}. \tag{10}$$

Here E_A is the Hartree-Fock energy of state A. To evaluate Eqs. (9) and (10), we must address the issue that the MOs of $|A^{(0)}\rangle$ and $|B^{(0)}\rangle$, $\{\phi_p^A\}$ and $\{\phi_p^B\}$, are mutually nonorthogonal.

Brute-force computation of the first term in Eqs. (9) and (10) would entail computing the determinant of the overlap matrix M_{ij}^{ab} for all excitations $(i, j) \to (a, b)$, where the overlap matrix elements are defined by $(M_{ij}^{ab})_{rs} = \langle\phi_r^A|\phi_s^B\rangle$ with ϕ_a^B and ϕ_b^B substituted for ϕ_i^B and ϕ_j^B, respectively. Evaluation of each determinant scales as N_{occ}^3, and this determinant must be evaluated for each $(i, j) \to (a, b)$ excitation, leading to an overall scaling of $N_{\text{occ}}^5 N_{\text{virt}}^2$ for the first term in Eq. (9). The second term on the RHS of Eq. (9) involves two sets of excitations, resulting in even steeper scaling.

To more efficiently evaluate the terms in Eqs. (9) and (10), we rotate the MOs and two-electron integrals for states A and B into a corresponding orbital basis.[66,67] In this basis, the occupied-occupied block of the overlap matrix, $(S)_{rs} = \langle\phi_r^A|\phi_s^B\rangle$, is diagonal, and the matrix elements of the overlap matrix become

$$\big\langle\phi_i^A\big|\phi_j^B\big\rangle = S_i\delta_{ij}, \tag{11}$$

$$\big\langle\phi_i^A\big|\phi_a^B\big\rangle = S_{ia}, \tag{12}$$

$$\big\langle\phi_a^A\big|\phi_i^B\big\rangle = S_{ai}. \tag{13}$$

This transformation greatly reduces the cost of evaluating the matrix elements in Eqs. (9) and (10), as shown below.

The overlap between $A^{(0)}$ and B_{ij}^{ab}, $\langle A^{(0)}|B_{ij}^{ab}\rangle$, in the corresponding orbital basis set is simply $\frac{1}{S_iS_j}\langle A^{(0)}|B^{(0)}\rangle(S_{ai}S_{bj} - S_{aj}S_{bi})$. Using the symmetry relations of the two-electron integrals and β_{ij}^{ab} amplitudes, the first term on the RHS of

Eq. (9) becomes

$$\frac{1}{4}E_A\langle A^{(0)}|B_{ij}^{ab}\rangle\beta_{ij}^{ab} = \frac{1}{2}E_A\frac{S_{ai}S_{bj}}{S_iS_j}\langle A^{(0)}|B^{(0)}\rangle\beta_{ij}^{ab}, \quad (14)$$

where $\langle A^{(0)}|B^{(0)}\rangle = \prod_k^N S_k$, and the resulting expression scales as $N_{\text{occ}}^2 \times N_{\text{virt}}^2$. An analogous procedure can be used to compute the remaining terms on the RHS of Eq. (9).

First we define the following two projected-overlap quantities in order to simplify the final set of equations,

$$S_{pr}^{ij} = \langle\phi_p^A|1 - \sum_{k\neq i,j}\frac{|\phi_k^B\rangle\langle\phi_k^A|}{S_k}|\phi_r^B\rangle, \quad (15)$$

$$S_{pr}^{i} = \langle\phi_p^A|1 - \sum_{k\neq i}\frac{|\phi_k^B\rangle\langle\phi_k^A|}{S_k}|\phi_r^B\rangle. \quad (16)$$

The expression for the overlap between doubly excited determinants $\langle A_{kl}^{cd}|B_{ij}^{ab}\rangle$ depends on how many occupied orbitals the states have in common, so we break up $\langle A_{kl}^{cd}|B_{ij}^{ab}\rangle$ into cases according to the number of common indices: (1) two common indices, $i = k$ and $j = l$; (2) one common index, $i = k$ and $j \neq l$; and (3) no common indices, $i \neq k$ and $j \neq l$. The simplified expression for the second term on the RHS of Eq. (9) is given below for each case.

Case 1. $i = k, j = l$:

$$\frac{1}{16}\langle kl\|cd\rangle_A\langle A_{kl}^{cd}|B_{ij}^{ab}\rangle\beta_{ij}^{ab} = \frac{1}{2}\frac{[\langle ij\|cd\rangle_A S_{ac}^{ij}][\beta_{ij}^{ab}S_{bd}^{ij}]\langle A^{(0)}|B^{(0)}\rangle}{S_iS_j}. \quad (17)$$

Case II. $i = k$, $j \neq l$:

$$\frac{1}{16}\langle kl\|cd\rangle_A\langle A_{kl}^{cd}|B_{ij}^{ab}\rangle\beta_{ij}^{ab} = \left[\frac{\langle il\|cd\rangle_A S_{ld}}{S_l}\right]\left[\frac{\beta_{ij}^{ab}S_{bj}}{S_j}\right]\frac{S_{ac}^i\langle A^{(0)}|B^{(0)}\rangle}{S_i} - \left[\frac{\langle ij\|cd\rangle_A S_{jd}}{S_j}\right]\left[\frac{\beta_{ij}^{ab}S_{bj}}{S_j}\right]\frac{S_{ac}^i\langle A^{(0)}|B^{(0)}\rangle}{S_i}. \quad (18)$$

Case III. $i \neq k$, $j \neq l$:

$$\frac{1}{16}\langle kl\|cd\rangle_A\langle A_{kl}^{cd}|B_{ij}^{ab}\rangle\beta_{ij}^{ab} = \frac{1}{4}\left[\frac{\langle kl\|cd\rangle_A S_{kc}S_{ld}}{S_kS_l}\right]\left[\frac{\beta_{ij}^{ab}S_{ai}S_{bj}}{S_iS_j}\right]\langle A^{(0)}|B^{(0)}\rangle - \left[\frac{\langle il\|cd\rangle_A S_{ic}S_{ld}}{S_iS_l}\right]\left[\frac{\beta_{ij}^{ab}S_{ai}S_{bj}}{S_iS_j}\right]\langle A^{(0)}|B^{(0)}\rangle + \frac{1}{2}\left[\frac{\langle ij\|cd\rangle_A S_{ic}S_{jd}}{S_iS_j}\right]\left[\frac{\beta_{ij}^{ab}S_{ai}S_{bj}}{S_iS_j}\right]\langle A^{(0)}|B^{(0)}\rangle. \quad (19)$$

The brackets are a visual aid to indicate where certain indices are pre-summed to reduce the scaling; for Eq. (17) the scaling is $N_{\text{occ}}^2N_{\text{virt}}^3$. The second term of Eq. (18) corrects for the fact that the implicit summation over i and j includes terms where $i = j$. We perform the full summation and then subtract the extra terms where $i = j$ instead of the restricted sum because this approach enables evaluation of Eq. (18) with only $N_{\text{occ}}^3N_{\text{virt}}^2$ effort. Likewise, the second and third terms in Eq. (19) correct for the inclusion of terms where $i = k$ and/or $j = l$ in the full summation, resulting in an expression that scales as $N_{\text{occ}}^2N_{\text{virt}}^2$. Finally, the second-order overlap matrix elements $\langle A^{(0)}|B^{(1)}\rangle$ can be recovered with no additional effort, as they are equal to the first term on the RHS of Eq. (9) divided by the energy E_A.

Equations (9)–(19) allow us to compute the matrix elements of the Hamiltonian and overlap matrix in the basis of perturbed HF states. A technical but nevertheless important practical consideration is the fact that some diagonal elements of the overlap matrix in the corresponding orbital basis, S_i, may be nearly zero, i.e., the overlap matrix may be singular. One way to circumvent the singular overlap matrix problem is to set all $|S_i|$ below a certain threshold with the value of the threshold, but this only is an approximate resolution of the problem. Instead, the derivation of Eqs. (14)–(19) may be modified to avoid the associated numerical instabilities. We have derived additional sets of equations, given in the supplementary material,[78] which specially address cases where some $S_i = 0$. These considerations do not increase the computational cost of the method, but they do increase the complexity of the equations.

The working equations of ΔSCF(2) presented above reveal that the cost of evaluating the ΔSCF(2) matrix elements scales at worst as $N_{\text{occ}}^2N_{\text{virt}}^3$, though the two electron integral transformations, which scale as N^5, end up being the slowest step in the ΔSCF(2) method. Since orbital optimization is implicit in the preparation of basis states for ΔSCF(2), the method does not require any simultaneous optimization of orbital coefficients and CI coefficients. This feature allows ΔSCF(2) to avoid the N^9 overlap diagonalization in CASPT2s. On the other hand, the substantial number of integral transforms required to evaluate Eqs. (17)–(19) in the corresponding orbital basis are a computational disadvantage relative to reduced active space approaches such as RASSCF. In ΔSCF(2), each non-Aufbau HF wavefunction must be determined self-consistently, so the number of HF calculations also grows as size of the active space squared, although this step is easily parallelized.

Given these expressions for the Hamiltonian and overlap matrix elements in the basis of perturbed ΔSCF states, we can diagonalize the Hamiltonian, i.e., solve Eq. (5) to obtain ΔSCF(2) energies and wavefunctions for the ground and excited states. In Sec. IV, we present results for some simple chemical systems and discuss the method's performance.

III. COMPUTATIONAL DETAILS

The ΔSCF(2) calculations use a modified version of Q-Chem 4.0,[68] and we use an in-house full CI code. The convergence of the ΔSCF states is aided where necessary by the maximum overlap method (MOM).[69] For systems where the size of the chosen basis set makes full CI prohibitively

expensive, we use the Rydberg-Klein-Rees[70,71] (RKR) method to calculate the experimental dissociation curve of the ground state with the RKR1 2.0 code.[72] The parameters used to produce the RKR potential for hydrogen fluoride can be found in a previous study by Coxon and Ogilvie.[73] For H_2, we use the cc-pVQZ basis set in order to approach the basis set limit within ΔSCF(2). The 6-311G basis set was used for H_4 calculations. In the case of hydrogen fluoride we employ the valence double-zeta Dunning-Hay basis set, as implemented in GAMESS.[74] The Dunning-Hay basis set makes a full CI computation feasible, permitting a comparison of ΔSCF(2) and full CI with a finite basis set for ground and excited states. We also use the cc-pVTZ basis set in order to compare with the RKR potential of hydrogen fluoride. The numerical data for H_2 and hydrogen fluoride can be found in the supplementary material.[78]

While the mixing of the ΔSCF states helps push the worst effects of the intruder-state problem away from the equilibrium geometry along the dissociation curve, it does not resolve the issue entirely. Therefore, to avoid intruder-state problems near dissociation in hydrogen fluoride and H_2 stemming from the PT2 correction[56] in Eq. (4), we replaced the denominator of Eq. (4), $\Delta\epsilon_A = \epsilon_a^A + \epsilon_b^A - \epsilon_i^A - \epsilon_j^A$, with a Lorentzian approximation that removes the divergence, $\frac{1}{\Delta\epsilon_A} \approx \frac{\Delta\epsilon_A}{\Delta\epsilon_A^2+\delta^2}$. Threshold values for the Lorentzian were chosen as small as possible while still ensuring a monotonically increasing ground state PES near the dissociation limit, resulting in values for δ of 0.3 hartree and 1.05 hartree for H_2 and hydrogen fluoride, respectively. No such modification was necessary for the H_4 calculations.

IV. EXCITED STATE POTENTIAL ENERGY SURFACES

To test this new approach to multireference PT2, we consider ground and low-lying excited states of the H_2, hydrogen fluoride, and tetrahedral H_4 molecules.

A. H_2 dissociation

The simplest realistic test case for multireference methods is dissociation of H_2: it has only two electrons, and at the dissociation limit it reduces to two one-electron systems. Natural basis states for the ΔSCF(2) method consist of the ground state, the α- and β-spin HOMO → LUMO non-Aufbau states, and the doubly excited HOMO → LUMO non-Aufbau state. The dissociation curves for both ΔSCF(2) and full CI are shown in Figure 1. The four different potential energy curves plotted are the ground state (S_0), lowest triplet state (T_1), singlet excited state (S_1), and the doubly excited state (S_2). One always obtains both the singlet and triplet excited states associated with a given one-electron excitation since they are simple linear combinations of the two broken-symmetry ΔSCF states, i.e., in the case of H_2 the HOMO → LUMO excited states. Like other multireference methods, ΔSCF(2) correctly describes the shape of the potential energy surfaces since its multireference nature captures most of the static correlation. We ascribe most of the discrepancy between ΔSCF(2) and full CI to the PT2-level description of dynamic correlation.[75,76]

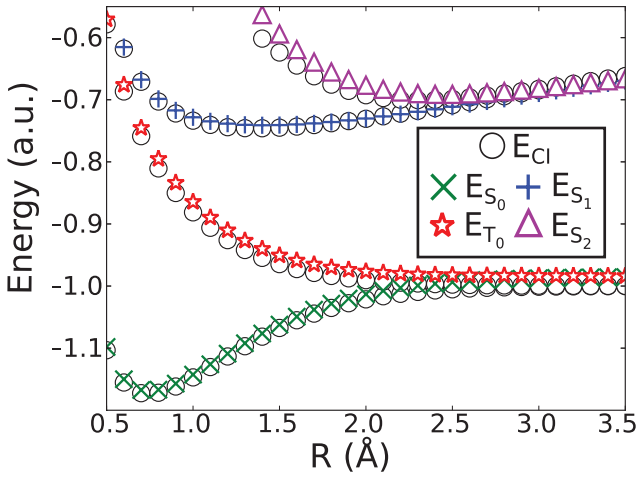

FIG. 1. H_2 dissociation potential energy curves computed with full CI (circles) and ΔSCF(2) in the cc-pVQZ basis. The ΔSCF(2) calculations included four states in total: the ground state, plus the singly and doubly excited HOMO → LUMO states. The ΔSCF(2) method performs well for the ground, singly, and doubly excited states over the entire potential energy surface.

The ΔSCF(2) excited states display accuracy similar to that of the ground state, with T_1 having the smallest mean absolute error (MAE) from full CI and S_2 having the largest MAE, shown in Table I. Also given in Table I is the non-parallelity error (NPE) from full CI, computed as NPE= avg($|\Delta E - \Delta E_{\text{avg}}|$), where ΔE is the difference between ΔSCF(2) and full CI energies. As the MAEs and NPEs given in Table I show, the ΔSCF(2) error grows as the basis set increases because of the increase in dynamic correlation correctly captured by full CI; but the error does not change much from the triple-zeta to the quadruple-zeta basis set. Overall ΔSCF(2) performs well for both the ground

TABLE I. Mean absolute errors (MAE) and non-parallelity errors (NPE, given in parentheses) of ΔSCF(2) from full CI, given in mhartree. Ground and excited state errors are of similar size, both for H_2 and for hydrogen fluoride.

H_2		**S_0**	**T_1**	**S_1**	**S_2**	
	cc-pVDZ	7.04 (2.14)	10.1 (0.60)	5.20 (4.80)	8.83 (8.37)	
	cc-pVTZ	8.73 (3.05)	13.7 (0.69)	4.51 (4.44)	13.2 (11.1)	
	cc-pVQZ	8.92 (3.45)	14.7 (1.23)	3.78 (3.78)	14.2 (12.3)	
FH		**$X^1\Sigma$**	**$^3\Pi$**	**$^1\Pi$**	**$^1\Sigma$**	**$^3\Sigma$**
	Dunning-Hay	8.51 (2.32)	12.7 (0.91)	11.4 (0.35)	12.8 (1.42)	16.9 (4.09)

and low-lying excited states of H_2 with a minimal number of HF states.

Interestingly, we find that the S_0 state from ΔSCF(2) lies above the full CI results by only 5 mhartree near the equilibrium distance yet rises to 14.5 mhartree above full CI at the dissociation limit, in contrast to what one would expect from errors due to dynamic correlation. For example, a (2,2) CASSCF calculation in the cc-pVQZ basis with no state-averaging has an error of 22 mhartree near equilibrium and less than 0.07 mhartree at the dissociation limit. As we will show for hydrogen fluoride, the lower error near equilibrium is because of the orbital relaxation in the ΔSCF states.

B. Hydrogen fluoride dissociation

We now turn to hydrogen fluoride as an exemplar for heteronuclear diatomic molecules since both its ground and excited states have been studied using a variety of multireference perturbation theory methods.[50,51,76] We consider the ground state, Σ singlet and triplet excited states, and Π singlet and triplet excited states of the hydrogen fluoride molecule. At equilibrium, the Σ excited states are made up of a transition from the σ bonding to anti-bonding orbitals. The Π excited states come from the degenerate p_x and p_y orbitals to the σ anti-bonding orbital. The wavefunction basis in the ΔSCF(2) calculations is made up of the HF ground state and nine ΔSCF states. Initial guesses for the nine ΔSCF states are constructed via two single-electron excitations and one two-electron excitation for each of the three relevant orbital transitions: $\sigma \rightarrow \sigma^*$ for the Σ state and p_x, $p_y \rightarrow \sigma^*$ for the Π states.

We start by computing the NPE of the ground state of hydrogen fluoride in the cc-pVTZ basis with the RKR potential energy surface, shown in Figure 2. For reference, the full CI

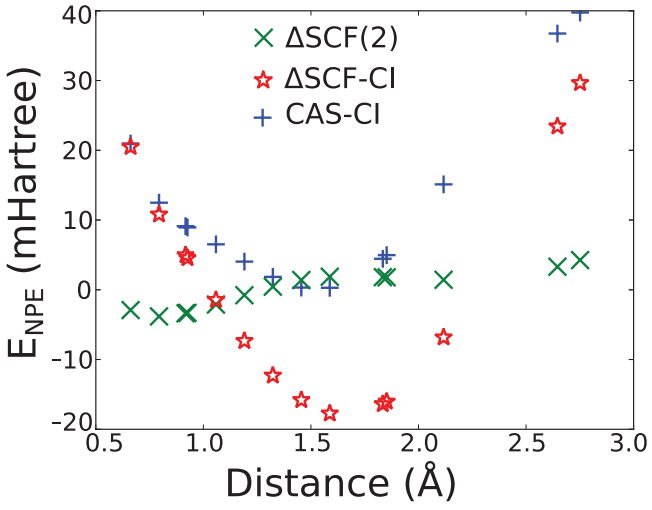

FIG. 2. Non-parallelity error of ΔSCF(2) (green), ΔSCF-CI (red), and CAS-CI (blue) computed in the cc-pVTZ basis with the Rydberg-Klein-Rees (RKR) potential for hydrogen fluoride. The non-parallelity error is defined in the text. All three methods include the same number of non-Aufbau states, but ΔSCF-CI includes no PT2 correction to the wavefunctions, and CAS-CI also does not include any orbital relaxation in the excited states. In order to emphasize the impact of orbital relaxation, both the ΔSCF-CI and CAS-CI curves are shifted by average error of ΔSCF-CI.

equilibrium bond distance for hydrogen fluoride is 0.917 Å. As in the case of H_2, the ΔSCF(2) ground state is closer to the RKR potential energy surface near equilibrium than at dissociation. To see if this behavior is due to the PT2 correction, orbital relaxation, or both, we compute the NPE for CAS-CI and for a PT2-free variant of ΔSCF(2), denoted ΔSCF-CI. The ΔSCF-CI values are computed using the same ΔSCF states as in the ΔSCF(2) calculations, but without any PT2 correction to the wavefunctions. The CAS-CI calculations consist of a CI calculation using the same initial non-Aufbau orbital occupations as in the ΔSCF(2) calculation, but without any excited state SCF orbital relaxation, i.e., the ground state orbitals are used for every state. In order to make the impact of orbital relaxation clearer, the CAS-CI curve is shifted by the same amount as the ΔSCF-CI curve (376 mhartree). The PT2 correction to the wavefunctions has a huge impact on the energies: the 376 mhartree error of ΔSCF-CI is lowered to 80 mhartree by ΔSCF(2). The ΔSCF(2) curve is also more parallel to the RKR surface because of the PT2 correction. Comparing the ΔSCF-CI and CAS-CI curves, we see that orbital relaxation is important near the equilibrium distance, which is why the ΔSCF(2) curve performs better near equilibrium than at dissociation for both H_2 and hydrogen fluoride.

We can compare ΔSCF(2) for the hydrogen fluoride ground state with two different CASPT2 calculations from Ref. 76. In Ref. 76 the authors compute the ground state of hydrogen fluoride using a valence and a 1:1 active space in the 6-31G** basis. The 1:1 active space consists of all occupied valence orbitals plus an active virtual orbital, of the same symmetry, for each occupied valence orbital. The valence active space for hydrogen fluoride has 8 electrons and 3011 active configurations per irreducible representation of the largest Abelian subgroup, and the 1:1 active space consists of 8 electrons and 4022 configurations. The average errors of CASPT2 in the valence and 1:1 active spaces are 8.2 and 5.6 mhartree, respectively. The average error in the ground state for ΔSCF(2) with a 10-wavefunction basis set is 10 mhartree, which is quite similar to the CASPT2 error despite the dramatically smaller number of reference determinants.

While the comparable performance of ΔSCF(2) and CASPT2 for the ground state is encouraging, its performance for excited states is the primary goal of this assessment. Moving onto the excited states, we plot the deviation of ΔSCF(2) from full CI using the Dunning-Hay basis in Figure 3. Overall, with a minimal set of 10 determinants, the ΔSCF(2) method stays fairly parallel to full CI for all states. The ΔSCF(2) method does not perform as well at short distances due to the increased dynamic correlation. Such larger errors at short distances have also been found for CASPT2 and CASSCF methods since the limited size of the active space makes it difficult to capture all of the dynamic correlation in this regime where core correlation can come into play.[50]

In Figure 3 we also see that the excited state errors are similar in size to errors in the ground state. The MAEs of ΔSCF(2) for the hydrogen fluoride molecule are between 11 and 17 mhartree, and the NPEs are between 0.3 and 4.0 mhartree, as detailed in Table I. While the MAEs are not smaller than those observed using alternative multireference

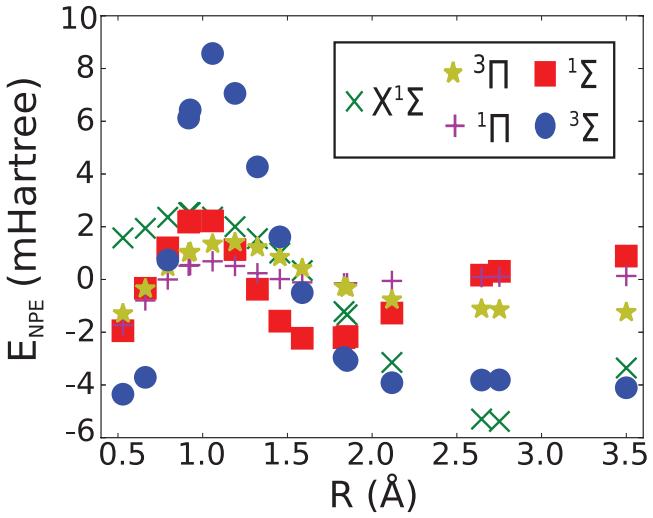

FIG. 3. Non-parallelity error, defined in the text, of the ΔSCF(2) potential energy from full CI for hydrogen fluoride as a function of bond length in the cc-pVTZ basis with 10 non-Aufbau states described in the text. Here $\Delta E = E_{\Delta SCF(2)} - E_{\text{Full-CI}}$. The ΔSCF(2) ground and excited state mean absolute errors vary between 8 and 17 mhartree. All of the states display greatest deviation from full CI near the equilibrium distance (0.917 Å) because of the approximate treatment of dynamic correlation in MP2.

methods,[51] the ΔSCF(2) method gives similar errors for all states using only 10 non-Aufbau basis states.

C. H4 conical intersection

The ability to describe and locate conical intersections is important for many practical applications, but remains a challenge for many excited state methods. To test the ability of ΔSCF(2) to describe conical intersections, we consider a minimal chemical model, the tetrahedral H_4 molecule. The conical intersection is located at the symmetric tetrahedral geometry. To treat the electronic structure at the conical intersection, we use a set of six non-Aufbau determinants that are symmetry-equivalent at the tetrahedral geometry. Plotted in Figure 4 are the ground state and lowest lying excited state potential energy surfaces of H_4 according to ΔSCF(2). As anticipated, since ΔSCF(2) is a "perturb then diagonalize" method, it is able to locate conical intersections as long as the degenerate states at the crossing are in the reference space.

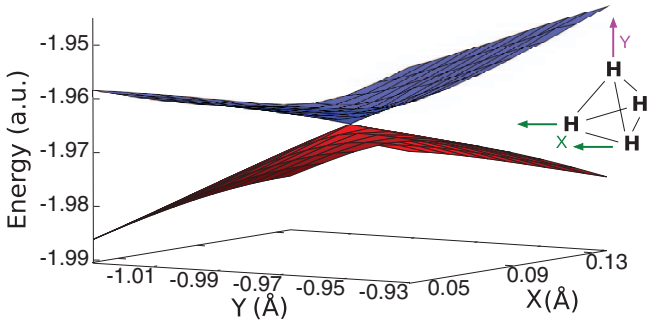

FIG. 4. ΔSCF(2) reproduces the conical intersection in the tetrahedral H_4 molecule in the 6-311G basis using six non-Aufbau states, with a non-parallelity error relative to full CI of 0.33 mhartree for the ground state. The inset on the right shows the definition of the X and Y coordinates.

For H_4 the MAE and NPE in the ground state are 7.4 and 0.33 mhartree, respectively. Just like in CAS methods, the error is generally reduced if the number of basis states (e.g., for CASSCF, the size of the active space) is increased. For example, if we add the HOMO → LUMO+1 double excitation and the HOMO → LUMO+2 double excitation to the H_2 ΔSCF(2) calculation in the cc-pVDZ basis, the difference with full CI at equilibrium goes from 5.7 mhartree to 2.4 mhartree. The energy at dissociation, however, still remains 10 mhartree above the full CI result. Because there is no state-averaging in ΔSCF(2), one can compute many excited states in one shot without sacrificing the accuracy of the ground state.

It should be noted that the ΔSCF(2) method is not a black box method because, as with the selection of an active space for CASPT2, one needs to choose a proper set of non-Aufbau HF reference states for ΔSCF(2). The ΔSCF(2) method is more useful when physical intuition, or simple methods like TDDFT, can be used to determine the desired excited state(s). That can greatly reduce the amount on ΔSCF states that need to be computed. Though one can also take the approach of computing all the ΔSCF states in a CAS type active space, or use a metadynamics based approach for locating multiple ΔSCF solutions.[33,77] For smaller molecules we have found that single excitations from a given state do not mix with that state, which can be used to reduce the number of ΔSCF states. Even though the orthogonality of the single excitations will break down for larger molecules, we expect these states to be redundant to include since the orbital relaxation in the ΔSCF states accounts for single excitations.

The test cases presented here show that there is promise for the ΔSCF(2) method for computing ground and excited state potential energy surfaces. The NPEs for the different molecular systems ranged from 0.3 to 12 mhartree for all the electronic states. Like CASPT2, we do not get all of the dynamic correlation when we use a small number of reference states. In the end we find the ΔSCF(2) method provides a new and potentially very accurate way to efficiently compute excited states in molecular systems.

V. CONCLUSION

Here we have presented a new multireference "perturb then diagonalize" strategy to obtain both static and dynamic correlations while treating ground and excited states even-handedly. The use of non-Aufbau ΔSCF wavefunctions for the excited states allows for the ground and excited states to have their own individually optimized set of molecular orbitals. Adding the perturbation before mixing the ground and excited state wavefunctions allows us to incorporate MP2 correlation in a state-specific manner. We have shown how to simplify the computation of matrix elements in this method such that terms scale no worse than $N_{\text{occ}}^2 \times N_{\text{virt}}^3$. By modeling a few simple systems we have found that the ΔSCF(2) method is able to locate conical intersections and to obtain ground and excited state potential energy surfaces to similar degrees of accuracy. ΔSCF(2) errors for these test systems are comparable to those from CASPT2 but are obtained using a substantially smaller space of reference wavefunctions.

Future work includes a direct implementation and parallelization of ΔSCF(2) into a computational chemistry package in order to take advantage of existing optimization techniques to accelerate ΔSCF(2) calculations. The nature of the ΔSCF(2) method also allows it to be parallelized in a semi-direct fashion. On a more fundamental level, as with other PT2 methods, ΔSCF(2) stands to benefit greatly from a non-empirical solution to the intruder state problem. Future work will explore the ΔSCF(2) description of excited states in larger and more complicated systems, such as open-shell radicals, in order to further asses the abilities and limitations of ΔSCF(2), though the present results already indicate the potential of ΔSCF(2) for modeling excited states with high accuracy.

ACKNOWLEDGMENTS

This work was funded by a grant from the National Science Foundation (Grant No. CHE-1058219).

[1]M. Fox and M. Chanon, *Photoduced Electron Transfer* (Elsevier, Amsterdam, 1988).
[2]C. Murphy, M. Arkin, Y. Jenkins, N. Ghatlia, S. Bossmann, N. Turro, and J. Barton, Science **262**, 1025 (1993).
[3]D. Ravelli, D. Dondi, M. Fagnoni, and A. Albini, Chem. Soc. Rev. **38**, 1999 (2009).
[4]W. Y. Teoh, J. A. Scott, and R. Amal, J. Phys. Chem. Lett. **3**, 629 (2012).
[5]N. Sariciftci, L. Smilowitz, A. Heeger, and F. Wudl, Science **258**, 1474 (1992).
[6]C. Brabec, A. Cravino, D. Meissner, N. Sariciftci, T. Fromherz, M. Rispens, L. Sanchez, and J. Hummelen, Adv. Funct. Mater. **11**, 374 (2001).
[7]C. J. Brabec, G. Zerza, G. Cerullo, S. De Silvestri, S. Luzzati, J. C. Hummelen, and S. Sariciftci, Chem. Phys. Lett. **340**, 232 (2001).
[8]A. Dreuw and M. Head-Gordon, Chem. Rev. **105**, 4009 (2005).
[9]R. McWeeny and B. T. Sutcliffe, *Methods of Molecular Quantum Mechanics*, 2nd ed. (Academic Press London, 1989).
[10]E. Runge and E. K. U. Gross, Phys. Rev. Lett. **52**, 997 (1984).
[11]E. K. U. Gross and W. Kohn, Phys. Rev. Lett. **55**, 2850 (1985).
[12]M. Wanko, M. Garavelli, F. Bernardi, T. A. Niehaus, T. Frauenheim, and M. Elstner, J. Chem. Phys. **120**, 1674 (2004).
[13]B. Kaduk and T. Van Voorhis, J. Chem. Phys. **133**, 061102 (2010).
[14]R. Peverati and D. G. Truhlar, Phys. Chem. Chem. Phys. **14**, 11363 (2012).
[15]O. A. Vydrov and T. Van Voorhis, J. Chem. Phys. **133**, 244103 (2010).
[16]J.-D. Chai and M. Head-Gordon, Phys. Chem. Chem. Phys. **10**, 6615 (2008).
[17]A. J. Cohen, P. Mori-Sánchez, and W. Yang, Chem. Rev. **112**, 289 (2012).
[18]B. O. Roos, K. Andersson, M. P. Fülscher, P. A. Malmqvist, L. Serrano-Andrés, K. Pierloot, and M. Merchán, Adv. Chem. Phys. **93**, 219 (1996).
[19]P. Pulay, Int. J. Quantum Chem. **111**, 3273 (2011).
[20]C. Møller and M. S. Plesset, Phys. Rev. **46**, 618 (1934).
[21]D. Cremer, WIREs Comput. Mol. Sci. **1**, 509 (2011).
[22]A. Szabo and N. S. Ostlund, *Modern Quantum Chemistry: Introduction to Advanced Electronic Structure Theory* (Dover Publications, 1996).
[23]R. J. Bartlett and M. Musiał, Rev. Mod. Phys. **79**, 291 (2007).
[24]M. Musiał, A. Perera, and R. J. Bartlett, J. Chem. Phys. **134**, 114108 (2011).
[25]J. F. Stanton and R. J. Bartlett, J. Chem. Phys. **98**, 7029 (1993).
[26]A. I. Krylov, Annu. Rev. Phys. Chem. **59**, 433 (2008).
[27]O. Christiansen, H. Koch, and P. Jørgensen, Chem. Phys. Lett. **243**, 409 (1995).
[28]C. Hättig and F. Weigend, J. Chem. Phys. **113**, 5154 (2000).
[29]J. A. Pople, M. Head-Gordon, and K. Raghavachari, J. Chem. Phys. **87**, 5968 (1987).
[30]K. Hirao, *Recent Advances in Multireference Methods* (World Scientific, 1999), Vol. 4.
[31]B. O. Roos, P. R. Taylor, and P. E. M. Siegbahn, Chem. Phys. **48**, 157 (1980).
[32]P. A. Malmqvist, A. Rendell, and B. O. Roos, J. Phys. Chem. **94**, 5477 (1990).
[33]A. J. Thom and M. Head-Gordon, J. Chem. Phys. **131**, 124113 (2009).
[34]K. Andersson, P. A. Malmqvist, B. O. Roos, A. J. Sadlej, and K. Wolinski, J. Phys. Chem. **94**, 5483 (1990).
[35]K. Andersson, P. A. Malmqvist, and B. O. Roos, J. Chem. Phys. **96**, 1218 (1992).
[36]K. Wolinski and P. Pulay, J. Chem. Phys. **90**, 3647 (1989).
[37]R. B. Murphy and R. P. Messmer, Chem. Phys. Lett. **183**, 443 (1991).
[38]K. Hirao, Chem. Phys. Lett. **190**, 374 (1992).
[39]P. M. Kozlowski and E. R. Davidson, J. Chem. Phys. **100**, 3672 (1994).
[40]J. J. McDouall, K. Peasley, and M. A. Robb, Chem. Phys. Lett. **148**, 183 (1988).
[41]K. Andersson, Theor. Chim. Acta **91**, 31 (1995).
[42]G. Ghigo, B. O. Roos, and P. A. Malmqvist, Chem. Phys. Lett. **396**, 142 (2004).
[43]K. G. Dyall, J. Chem. Phys. **102**, 4909 (1995).
[44]C. Angeli, R. Cimiraglia, S. Evangelisti, T. Leininger, and J.-P. Malrieu, J. Chem. Phys. **114**, 10252 (2001).
[45]B. Kirtman, J. Chem. Phys. **75**, 798 (1981).
[46]J. Malrieu, P. Durand, and J. Daudey, J. Phys. A **18**, 809 (1985).
[47]B. Brandow, Int. J. Quantum Chem. **15**, 207 (1979).
[48]J. Paldus and X. Li, Adv. Chem. Phys. **110**, 1 (1999).
[49]J. Pittner, P. Nachtigall, P. Čársky, J. Mášik, and I. Hubač, J. Chem. Phys. **110**, 10275 (1999).
[50]A. Engels-Putzka and M. Hanrath, J. Mol. Struct.: THEOCHEM **902**, 59 (2009).
[51]V. V. Ivanov, L. Adamowicz, and D. I. Lyakh, J. Mol. Struct.: THEOCHEM **768**, 97 (2006).
[52]T. Mori and S. Kato, Chem. Phys. Lett. **476**, 97 (2009).
[53]N. Handy, P. Knowles, and K. Somasundram, Theor. Chim. Acta **68**, 87 (1985).
[54]J. Olsen, O. Christiansen, H. Koch, and P. Jørgensen, J. Chem. Phys. **105**, 5082 (1996).
[55]J. Olsen, P. Jørgensen, T. Helgaker, and O. Christiansen, J. Chem. Phys. **112**, 9736 (2000).
[56]C. D. Sherrill, Annu. Rep. Comp. Chem. **1**, 45 (2005).
[57]C. Camacho, H. A. Witek, and S. Yamamoto, J. Comput. Chem. **30**, 468 (2009).
[58]M. R. Hoffmann, D. Datta, S. Das, D. Mukherjee, A. Szabados, Z. Rolik, and P. Surjan, J. Chem. Phys. **131**, 204104 (2009).
[59]M. P. Deskevich, D. J. Nesbitt, and H.-J. Werner, J. Chem. Phys. **120**, 7281 (2004).
[60]H.-J. Werner and P. J. Knowles, J. Chem. Phys. **89**, 5803 (1988).
[61]P. Celani and H.-J. Werner, J. Chem. Phys. **112**, 5546 (2000).
[62]T. Kowalczyk, S. R. Yost, and T. Van Voorhis, J. Chem. Phys. **134**, 054128 (2011).
[63]M. W. D. Hanson-Heine, M. W. George, and N. A. Besley, J. Chem. Phys. **138**, 064101 (2013).
[64]T. Ziegler, A. Rauk, and E. J. Baerends, Theor. Chim. Acta **43**, 261 (1977).
[65]S. C. Leasure and G. G. Balint-Kurti, Phys. Rev. A **31**, 2107 (1985).
[66]A. T. Amos and G. G. Hall, Proc. R. Soc. London, Ser. A **263**, 483 (1961).
[67]H. F. King, R. E. Stanton, H. Kim, R. E. Wyatt, and R. G. Parr, J. Chem. Phys. **47**, 1936 (1967).
[68]Y. Shao, L. F. Molnar, Y. Jung, J. Kussmann, C. Ochsenfeld, S. T. Brown, A. T. B. Gilbert, L. V. Slipchenko, S. V. Levchenko, D. P. O'Neill, R. A. DiStasio, R. C. Lochan, T. Wang, G. J. O. Beran, N. A. Besley, J. M. Herbert, C. Y. Lin, T. Van Voorhis, S. H. Chien, A. Sodt, R. P. Steele, V. A. Rassolov, P. E. Maslen, P. P. Korambath, R. D. Adamson, B. Austin, J. Baker, E. F. C. Byrd, H. Dachsel, R. J. Doerksen, A. Dreuw, A. Dunietz, A. Heyden, S. Hirata, C. P. Hsu, G. Kedziora, R. Z. Khalliulin, P. Klunzinger, A. M. Lee, M. S. Lee, W. Liang, I. Lotan, N. Nair, B. Peters, E. I. Proynov, P. A. Pieniazek, Y. M. Rhee, J. Ritchie, E. Rosta, C. D. Sherrill, A. C. Simmonett, J. E. Subotnik, H. L. Woodcock, W. Zhang, A. T. Bell, A. K. Chakraborty, D. M. Chipman, F. J. Keil, A. Warshel, W. J. Hehre, H. F. Schaefer, J. Kong, A. I. Krylov, P. M. W. Gill, and M. Head-Gordon, Phys. Chem. Chem. Phys. **8**, 3172 (2006).
[69]N. A. Besley, A. T. Gilbert, and P. M. Gill, J. Chem. Phys. **130**, 124308 (2009).
[70]A. Rees, Proc. Phys. Soc. London **59**, 998 (1947).
[71]A. Hurley, J. Chem. Phys. **36**, 1117 (1962).
[72]R. Le Roy, RKR1 2.0: A Computer Program Implementing the First-Order RKR Method for Determining Diatomic Molecule Potential Energy Curves, University of Waterloo Chemical Physics Research Report CP-657R (2004); available online http://leroy.uwaterloo.ca.

[73]J. Coxon and J. Ogilvie, Can. J. Spectrosc. **34**, 137 (1989).
[74]M. W. Schmidt, K. K. Baldridge, J. A. Boatz, S. T. Elbert, M. S. Gordon, J. H. Jensen, S. Koseki, N. Matsunaga, K. A. Nguyen, S. Su, T. L. Windus, M. Dupuis, and J. A. Montgomery, Jr., J. Comput. Chem. **14**, 1347 (1993).
[75]B. O. Roos, Adv. Chem. Phys. **69**, 399 (1987).
[76]M. L. Abrams and C. D. Sherrill, J. Phys. Chem. A **107**, 5611 (2003).
[77]A. J. W. Thom and M. Head-Gordon, Phys. Rev. Lett. **101**, 193001 (2008).
[78]See supplementary material at http://dx.doi.org/10.1063/1.4827456 for ΔSCF(2) equations for the case of one or more $S_i = 0$. As well as numerical data for H_2 and FH.